

Article

# Estimation of Phase Noise Transfer Function †

Igor Rutkowski \*  and Krzysztof Czuba 

Institute of Electronic Systems, Warsaw University of Technology, 00-665 Warsaw, Poland;  
krzysztof.czuba@pw.edu.pl

\* Correspondence: I.Rutkowski@elka.pw.edu.pl

† This paper is an extended version of our paper published in 2020 23rd International Microwave and Radar Conference (MIKON) under the title “Characterization of Frequency Converters’ Phase Noise Transfer Function”, Warsaw, Poland, 5–8 October 2020; pp. 1–4, doi:10.23919/MIKON48703.2020.9253777.

**Abstract:** Quantifying frequency converters’ residual phase noise is essential in various applications, including radar systems, high-speed digital communication, or particle accelerators. Multi-input signal source analyzers can perform such measurements out of the box, but the high cost limits their accessibility. Based on an analysis of phase noise transmission theory and the capabilities of popular instrumentation, we propose a technique extending the functionality of single-input devices. The method supplements absolute noise measurements with estimates of the phase noise transfer function (also called the jitter transfer function), allowing the calculation of residual noise. The details of the hardware setup used for the method verification are presented. The injection of single-tone and pseudo-random modulations to the test signal is examined. Optional employment of a spectrum analyzer can reduce the time and number of data needed for characterization. A wideband synthesizer with an integrated voltage-controlled oscillator was investigated using the method. The estimated transfer function matches a white-box model based on synthesizer’s structure and values of loop components. The first results confirm the validity of the proposed technique.

**Keywords:** phase noise; frequency synthesis; RF device modeling and characterization



**Citation:** Rutkowski, I.; Czuba, K. Estimation of Phase Noise Transfer Function †. *Energies* **2021**, *14*, 8234. <https://doi.org/10.3390/en14248234>

Academic Editors: Gian Piero Gibiino and Corrado Florian

Received: 19 October 2021  
Accepted: 1 December 2021  
Published: 7 December 2021

**Publisher’s Note:** MDPI stays neutral with regard to jurisdictional claims in published maps and institutional affiliations.



**Copyright:** © 2021 by the authors. Licensee MDPI, Basel, Switzerland. This article is an open access article distributed under the terms and conditions of the Creative Commons Attribution (CC BY) license (<https://creativecommons.org/licenses/by/4.0/>).

## 1. Introduction

When a periodic signal passes through an electronic device, the extra fluctuations added to its phase are known as the additive (or residual) phase noise (PN). Puglia [1] provides “derivations and techniques applicable to a mathematical analysis model of the degradation in phase noise-to-carrier ratio of various components and cascade of components”. An assumption of full transmission of the input PN is made, which is valid for the classes of components examined (amplifiers, passive components, and frequency multipliers). For certain other types of devices, the input PN is only partially transferred, and different models are needed. Egan [2] investigated “processing of noise modulation by the phase-locked loop” (PLL) and described the total PN at the device output as:

$$\phi_{tot} = \phi_{res} + H(s) * \phi_{in} = \phi_{res} + \phi_{out} \quad (1)$$

where  $\phi_{tot}$  is the total PN at the device output,  $\phi_{res}$  is the residual PN at the device output,  $\phi_{in}$  is the PN at the device input, and  $\phi_{out} = H(s) * \phi_{in}$  is the input PN partially transferred to the output. In this paper, the phase noise transfer function (PNTF) is defined as

$$H(s) = \frac{\phi_{tot} - \phi_{res}}{\phi_{in}} \quad (2)$$

The term was primarily used for analyzing PLLs (for example, in [2,3]) but can be generalized to characterize all types of synthesizers and frequency converters. The additive part can be measured, or it can be calculated, when all three of the following are known:

- the PNTF;
- the absolute output noise;
- the absolute input noise.

Having discussed the theoretical foundations, we focus on the PN measurements next.

### 1.1. Phase Noise Measurement Instrumentation and Setups

Various techniques were developed to quantify the PN. In the most straightforward method, a spectrum analyzer (SA) detects the power spectral density around the carrier of interest. Another approach mixes the signal with its delayed copy. The last method derives information from comparing the phase of the input signal with a low-noise oscillator phase-locked to it. Both the second and third techniques employ a baseband analyzer.

The first setups were purpose built, and integrated PN measurement systems became available later. Cross-spectrum measurement is a technique improving the noise floor of signal source analyzers (SSAs), and it can be used in devices with at least two receivers. Gruson [4] reported on artifacts generated by popular implementations of the method.

Single-input instruments (for example, Rhode and Schwarz FSUP or Keysight E5052A/B) determine the absolute PN only. The measurement of residual PN is performed using more complicated setups, such as shown in [5]. If the period remains the same (for example, in an amplifier), the signals at the input (reference) and the output of a device under test (DUT) can be compared. In the case of frequency converters, the output signals of two DUTs (synchronized to the same reference) are mixed, and the baseband signal is analyzed.

Recently introduced multi-input SSAs (such as Rhode and Schwarz FSWP or Holtzworth HA7062C) can automatically separate the additive PN, even for frequency converters (e.g., [6]). Many laboratories are not yet equipped with new instrumentation because of its high cost. This research aimed to extend the functionality of more widely available single-input equipment. The additive PN can be calculated according to Equation (2), if the exact transfer function is determined. In many cases, it is not. Schemes for obtaining the unknown PNTF are discussed next.

### 1.2. Phase Noise Transfer Function Quantification

PNTF is often measured in high-speed serial communication, where the clock recovery circuit in a transceiver includes a PLL and extracts the timing information from the serial data stream. The PNTF, often called jitter transfer function (JTF) in the digital domain, can be evaluated using dedicated test equipment such as SV1C personalized SerDes tester <https://introspect.ca/product/sv1c-8/> (accessed on 30 November 2021) or in purpose-built setups utilizing oscilloscopes or SAs. To the best of the authors' knowledge, there is only one publication on measuring the PNTF (JTF) with SSA—our conference paper [7]. This article significantly extends research described in the conference publication. SSA offers better accuracy of close-to-carrier spectral components compared to instrumentation used for digital circuits.

The simplified block diagram of the setup for the method is presented in Figure 1. The input of the investigated device is stimulated with a signal (further called the test signal) consisting of a carrier with a defined phase modulation (injected signal). For the residual PN much weaker than the spur, Equation (2) simplifies to

$$H(s) = \frac{\phi_{out}}{\phi_{in}} = \frac{\phi_{tot} - \phi_{res}}{\phi_{in}} \stackrel{\phi_{tot} \gg \phi_{res}}{\approx} \frac{\phi_{tot}}{\phi_{in}} \quad (3)$$

The phase of the PNTF can be discarded, and its magnitude equals (for  $s = j\omega$ )

$$|H(j\omega)| = \frac{L_{out}(f)}{L_{in}(f)} \quad (4)$$

where  $L_{out}(f)$  and  $L_{in}(f)$  are the spur levels relative to the carrier in the output and input signals, respectively. In decibels,

$$PNTF(f) = 20 * \log_{10}(|H(j2\pi f)|^2) = 20 * \log_{10}(L_{out}(f)) - 20 * \log_{10}(L_{in}(f)) \quad (5)$$

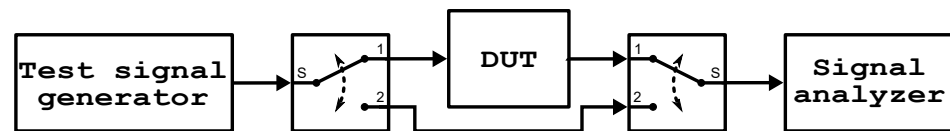


Figure 1. The block diagram of a test setup for characterization of the phase noise transfer function.

Single-channel instrumentation can be used to estimate the PNTF, and only one DUT is needed for such characterization. When the DUT converts the frequency, the translation effects must be corrected for. The amplitude modulation to phase modulation conversion effect is not taken into account in this simplified model.

In the second step, the modulation is turned off, or the reference generator is replaced, and the absolute output PN is measured. When the two are known, the residual PN can be calculated.

Having discussed the theoretical basis of the proposed method, we discuss synthesizers, which make up one of the essential classes of frequency converters.

### 1.3. Synthesizers

Synthesizers may be classified into three types:

- direct analog;
- direct digital;
- indirect digital.

The direct analog approach uses frequency dividers, mixers, and filters to produce and select the desired spectral component at the mixer's output. Within the band-pass, the device closely follows the PN of the reference, with the additional noise induced by the divider and the mixer. The PNTF is determined by the band-pass filter.

A direct digital synthesizer (DDS) uses a numerically controlled oscillator (NCO) feeding a digital-to-analog converter (DAC), both synchronized by the same clock. Many of the integrated circuits (ICs) available on the market include PLLs. When the PLL is not used, the PNTF is defined by the DAC reconstruction filter.

An indirect digital synthesizer utilizes a PLL with an integer or fractional frequency divider. For simplicity, we consider only a passive filter. Within the loop bandwidth, the PN comes from three sources: the reference, the phase detector, and the filter elements [2]. Outside this bandwidth, the noise is dominated by the voltage-controlled oscillator (VCO) and the optional output divider.

The PNTFs of synthesizers vary greatly in corner frequency and steepness. A method for analyzing them is discussed in the next section.

## 2. Materials and Methods

### 2.1. Test Signal Generation

The PNTF characterization method proposed in Section 1.2 needs a test signal, which can be obtained in various ways. A generator with a built-in phase modulator is the most convenient source. When such equipment is not present, different hardware must be employed. The most straightforward schemes include:

- a DDS IC with phase modulation capability;
- a vector modulator;
- a locked PLL with a spur injected to the control signal of a VCO.

This research was limited to DDS, as necessary components were available. A comprehensive overview of the theory concerning such devices can be found in [8]. When a

modulating input is present, the digital words are fed by an external digital circuit such as a field-programmable gate array (FPGA) device. The injected signal should be weak enough compared to the carrier to allow small-signal analysis but sufficiently strong to be easily detectable by the instrumentation (remain above the PN of a synthesizer). The magnitude is set by selecting the number of least significant bits modulated or by the programmable gain (if available). The number of bits affects the quantization error and the signal-to-noise-and-distortion (SINAD) ratio. The carrier is considered direct current (DC).

A 1 GSPS DDS made by analog devices (AD9910) was used to investigate the method. It integrates a 14-bit 1 GSPS DAC, and it can be modulated using a 16-bit word provided at the parallel port. An external 1 GHz reference was used as the system clock. The output frequency was set to 125 MHz, while the external data were sampled at 250 MHz. The modulating data were sourced by the firmware running on the Artix-7 FPGA (part of the Arty A7 development board <https://reference.digilentinc.com/reference/programmable-logic/artix-a7/start> (accessed on 30 November 2021)). A single tone adds two desired spectral components (positive and negative), and a separate measurement is required for each sweep point. Schat and Möhlmann [9] proposed stimulating a PLL with pseudo-random noise superimposed to the input clock signal, making a simultaneous measurement of the PNTF in the whole band of interest possible. Their research was limited to simulation. We investigate both types of modulation.

#### 2.1.1. Sinewave Modulation

With a constant data rate, the minimal spur frequency depends on the length of NCO's sinewave table. The operator can adjust the NCO step to increase the actual frequency. No programmable phase modulation gain is available; therefore, the amplitude was set by selecting only the eight lowest bits in the parallel input data bus. The maximum table length was limited to 64K by the FPGA resources, corresponding to 3.81 kHz.

Figure 2 shows the PN spectra of the test signal ( $20 * \log_{10}(L_{in}(f))$  in Equation (5)) at the AD9910 DDS output for selected sine table lengths (with display mode set to spur power). Measurements were performed using the Keysight E5052B, <https://www.keysight.com/en/pd-1081579-pn-E5052B/ssa-signal-source-analyzer-10-mhz-to-7-ghz-265-ghz-or-110-ghz> (accessed on 30 November 2021), the only SSA available to our team. The amplitude of the intended spur is independent of the offset frequency. Due to the small digital word resolution, the harmonics of each sinewave limit the SINAD to only 33 dB, corresponding to 5.5 ENOB, which is much less than the 8 bits used. However, the DAC resolution is 2 bits smaller than the data width and limits the ENBOB to 6 bits.

The spurs present in the amplitude modulation (AM) spectrum (Figure 3) might be caused by this restricted resolution or by the phase modulation to amplitude modulation (PM-to-AM) conversion in the SSA itself. The manufacturer does not quantify this conversion effect in the available documentation. The observed conversion increases with the offset frequency and becomes positive (the AM spur is stronger than the PM spur) for the second harmonic of the fastest modulation measured.

Due to SSA's logarithmic sweep (which cannot be changed by the user), the width of the spectrum bin increases with the offset frequency. The distance between harmonics/sidebands can become comparable to this width. When neighboring bins cover two or more harmonics, the SSA does not correctly report the spurs' power, which affects the detection of far-from-carrier harmonics. In the case of sinewave, however, we are interested only in detecting the level of the fundamental, which is always easily distinguishable.

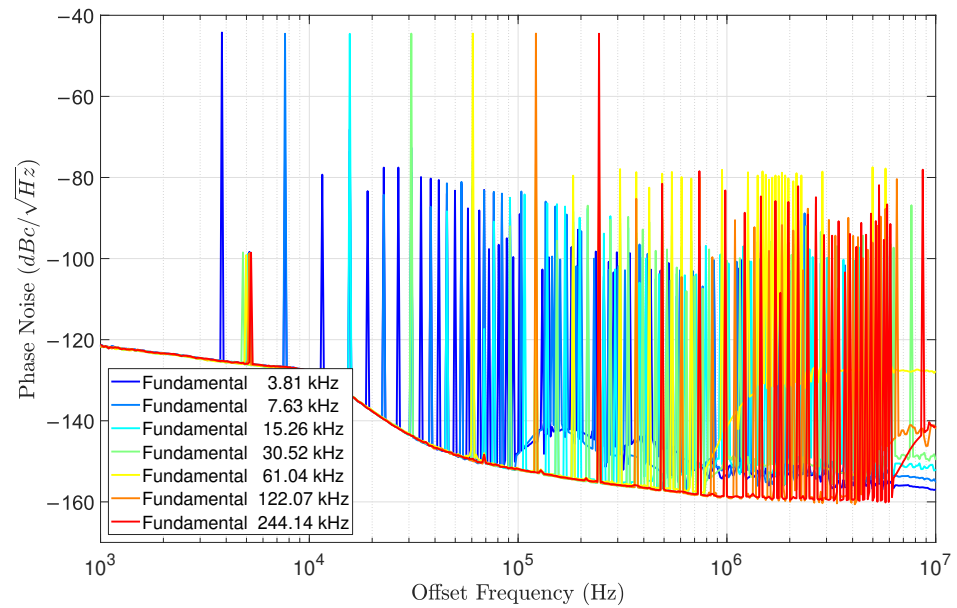


**Figure 2.** The phase noise spectra of the sinewave modulated test signals generated using the AD9910 DDS for various fundamental frequencies. Reprinted with permission from ref. [7]; Copyright 2021 IEEE.

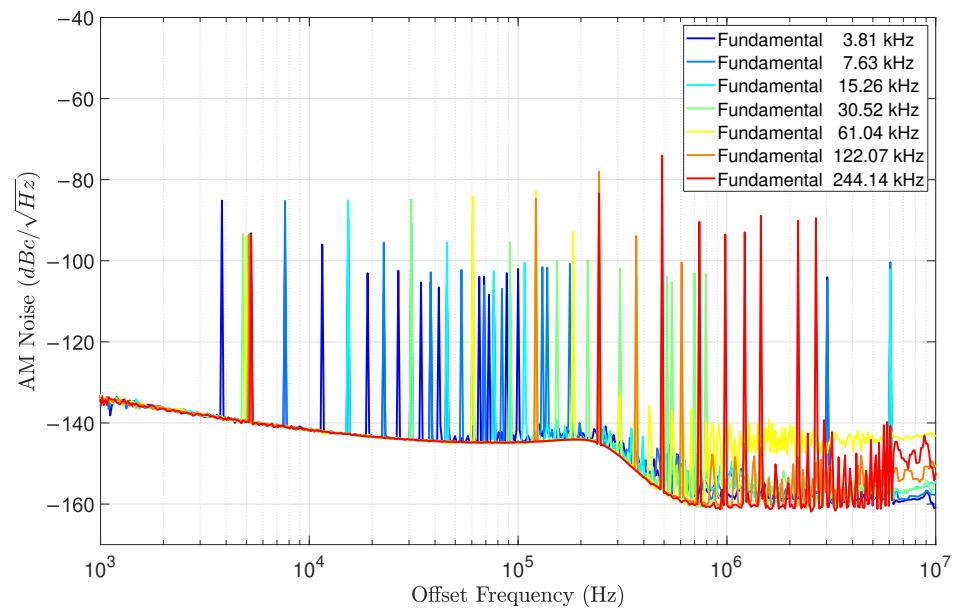


**Figure 3.** The AM noise spectra of the sinewave modulated test signals generated using the AD9910 DDS for various fundamental frequencies.

SAs offer linear sweeps and hence can distinguish far-from-carrier components. Their ability to discriminate weak and close-to-carrier components is limited. SAs cannot distinguish the type of modulation performed, only the magnitude of the spectral components. The spectrum was also measured using the Keysight N9030A SA with the following settings:

- 1 MHz span;
- 5001 points;
- 200 Hz resolution bandwidth.

The detected fundamental levels (not shown) were very similar to the SSA results. Both types of instrumentation can be used with the sinewave modulated signal.

### 2.1.2. Pseudo-Random Modulation

Linear feedback shift registers (LFSR) are simple pseudo-random generators, which can produce a repeatable sequence of numbers with statistical properties similar to that of noise [10]. Different LFSRs are available; some minimize the sample correlation, while others minimize the number of resources used. An N-bit maximum-length LFSR generates a sequence covering all values between  $2^N - 1$  and 1. The modulation strength can be set by changing the number of LFSR's output bits used.

A 15-bit maximum-length LFSR generator was selected as an example. The magnitude of the Fourier transform of the digital output signal is presented in Figure 4. The spectra are not constant, but in the band surrounding the DC point, they are uniform enough to be used for device characterization. For eight or more output bits enabled, the 3dB cut-off frequency is 0.015, corresponding to 3.75 MHz for the selected generator configuration.

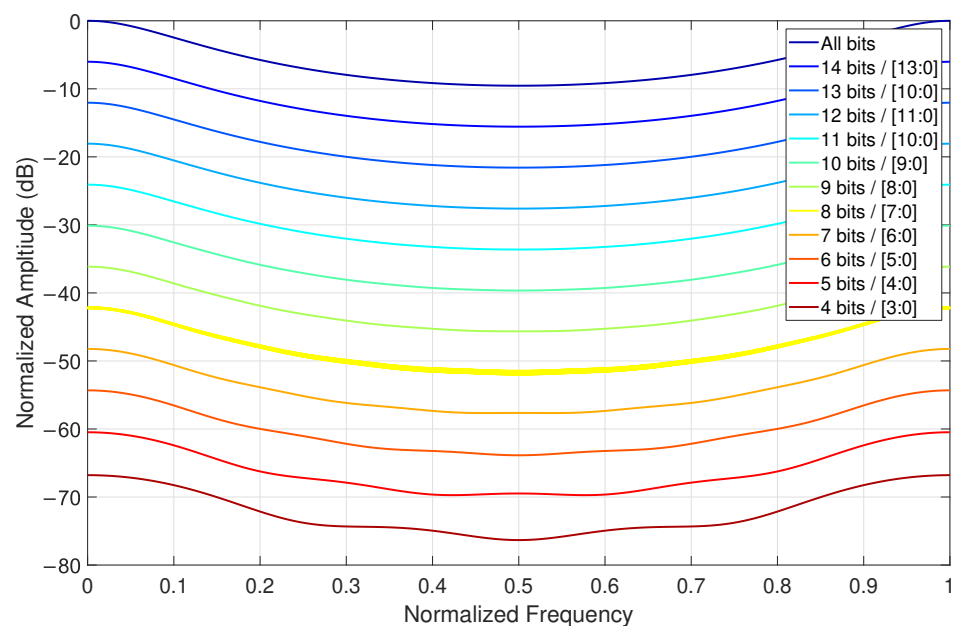


**Figure 4.** The magnitude of Fourier transform of 15 bit maximum-length LFSR generator output signal (DC value omitted).

The PN spectra of the analog test signal with the LFSR modulation injected are shown in Figure 5.

In the hundred kHz range, the spacing of the sidebands (7.63 kHz) becomes comparable to the width of the spectrum bins rendering the proper detection of each harmonic level impossible. The AM noise spectrum (not shown) was similarly affected.

The test signal was also measured using an SA. The power levels of spectral components (as a single sideband) were extracted from the spectra (see Figure 6) to improve readability. When 10–15 bits are used, the maximum deviation from the mean value is smaller than 5.5 dB. These configurations were selected for further usage. The pseudo-random modulation should only be measured with an SA, which correctly detects far-from-carrier components, unlike an SSA.

Testing with sinewave offers a slight advantage over using LFSR-generated patterns (SINAD of only 33 dB) but requires a separate measurement for each sweep point and lasts much longer. Therefore, the latter approach was used for the characterization of a DUT.

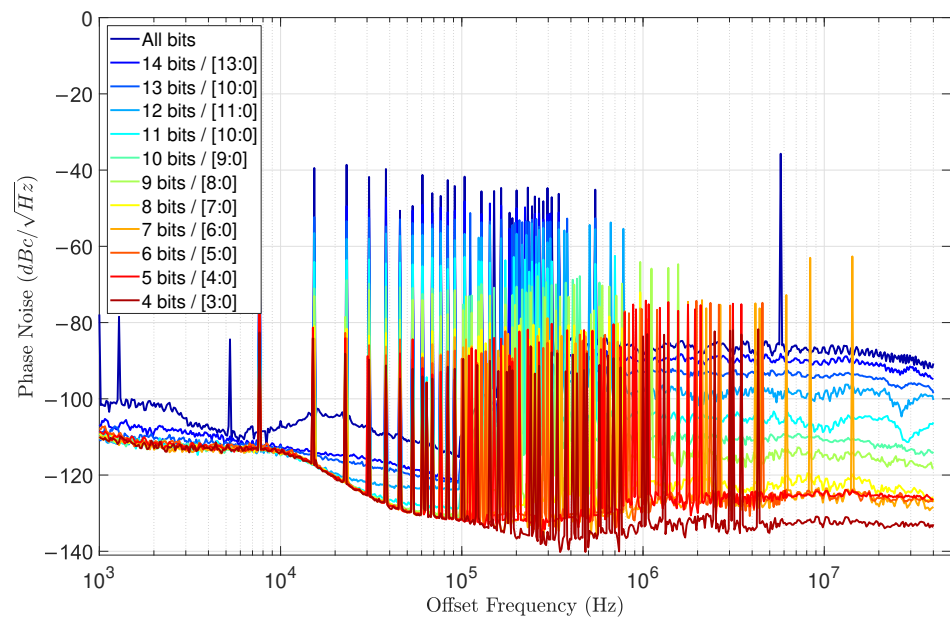


**Figure 5.** The PN spectra of the 15-bit maximum-length LFSR modulated test signals generated using the AD9910 DDS.

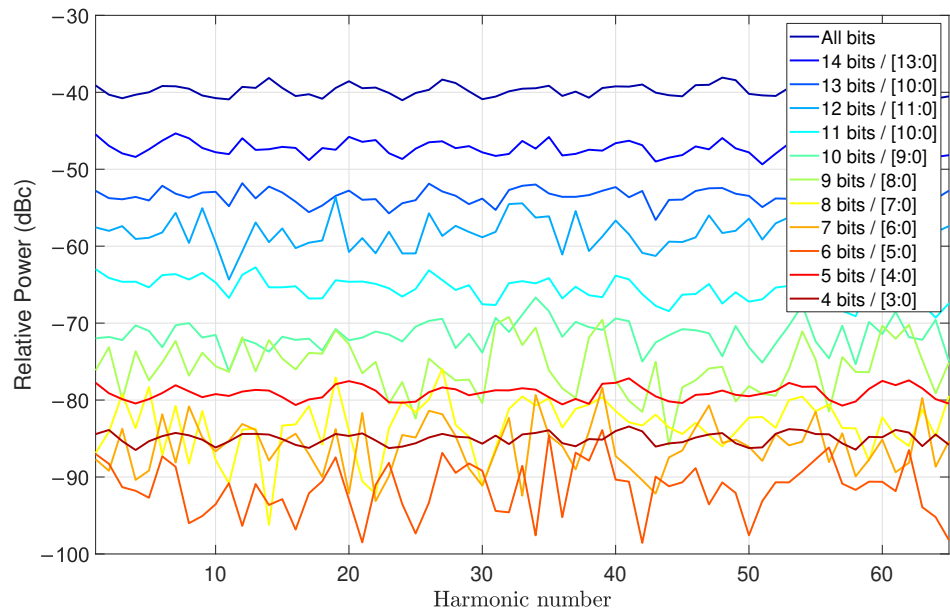


**Figure 6.** The relative power levels of sidebands in the 15 bit maximum-length LFSR modulated test signals generated using the AD9910 DDS.

### 3. Results

A wideband synthesizer with an integrated VCO (LMX2592, <http://www.ti.com/product/LMX2592> (accessed on 30 November 2021) made by Texas Instruments) was the DUT. The effective loop filter characteristic can be adjusted programmatically by changing the charge pump current. The filter components remained at stock values of the evaluation module (LMX2592EVM, <https://www.ti.com/tool/LMX2592EVM> (accessed on 30 November 2021)). A white-box model was built based on the synthesizer's structure (including the degree of filter, current to voltage conversion effects, and feedback type) and the nominal values of the filter components, with only one parameter unknown—the controller's gain.

The research began with an investigation of the undisturbed PLL for the selected charge pump current values. The Rhode Schwarz SMB100B generator synthesized a

125 MHz reference. The VCO operated at 4 GHz, and the output division ratio was set to 4. The high fidelity of the reference renders the noise added by the PLL visible. The PN of the DUT is significantly higher within the loop bandwidth than for the frequency-translated 125 MHz reference (see Figure 7). Low-charge pump currents allow us to observe the high offset frequency noise, which has a slope of approximately  $-20$  dB per decade and originates in the VCO or the output section. For high currents, the close-to-carrier noise has a slope of  $-10$  dB per decade and comes from the phase detector, the input circuits, or the charge pump. Spikes between 7 and 150 kHz correspond to the cut-off frequency, and their location is linearly proportional to the current.

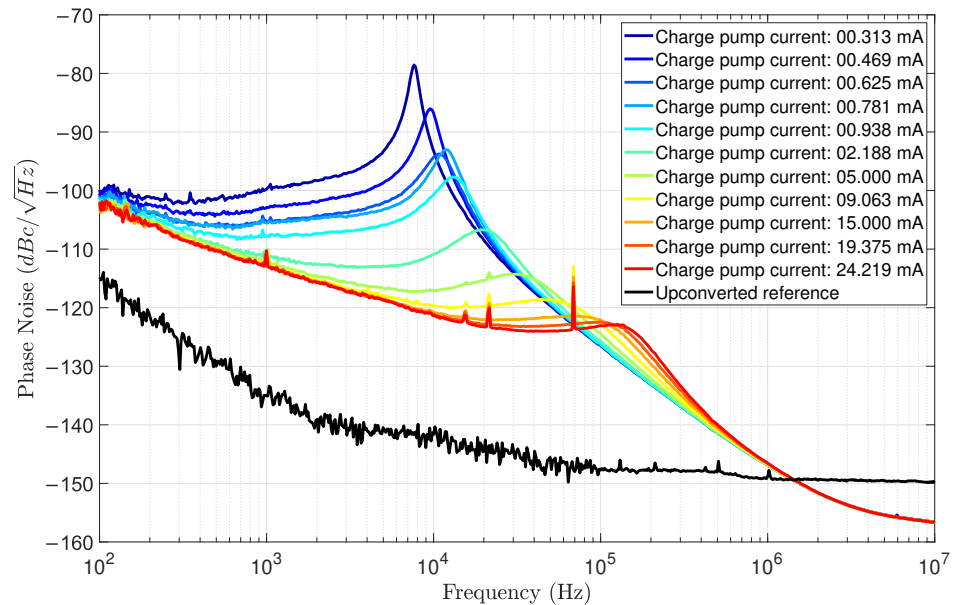


**Figure 7.** The phase noise spectra of frequency translated reference signal and unmodulated signal at the LMX2592 output for a range of charge pump current values. Reference frequency 125 MHz, output frequency 1 GHz, and VCO frequency 4 GHz. Reprinted with permission from ref. [7]; Copyright 2021 IEEE.

The manufacturer provides a simulation tool called PLLatinum Sim <https://www.ti.com/tool/PLLATINUMSIM-SW> (accessed on 30 November 2021), which can simulate the output PN as well as the internal transfer functions of the selected device. The measured spectra (Figure 7) differ significantly from the calculated by the software (not shown); therefore, the white-box model could not be determined this way.

Figure 8 presents the measured PNTFs (a black box model) of the selected DUT. The white-box model was fitted to the same data. The characteristics obtained using the proposed method (solid lines with dots) match the physically constrained curve (dashed lines) well, with the largest absolute difference reaching 3.5 dB for one point (the first sideband for 0.625 mA charge pump current) and not exceeding 2 dB for all other points.

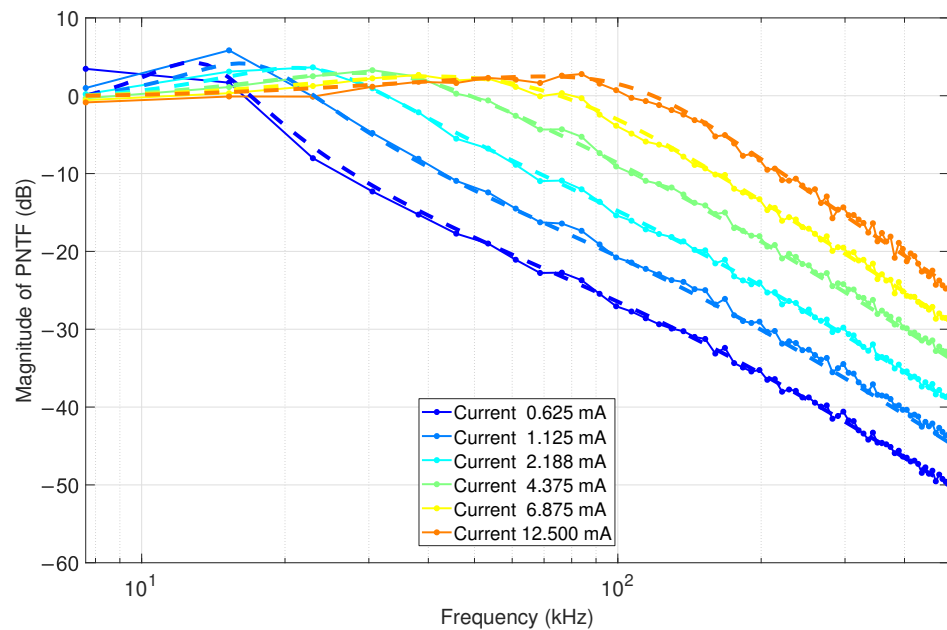


**Figure 8.** The magnitude of the measured (solid lines with dots) and modeled (dashed lines) PNTF characteristics of the LMX2592 for the selected charge pump current values. Reference frequency 125 MHz, output frequency 1 GHz, and VCO frequency 4 GHz.

#### 4. Conclusions

This paper proposes a method for measuring PN transmission using single-input SSAs, which has not been described in the literature so far. The injection of sinewave and pseudo-random modulations to the test signal was examined, with the latter deemed incompatible with SSA. A wideband synthesizer was characterized with the technique. The measurements match well the white-box model based on the physical structure of the DUT (including the values of loop components). The empirical findings show that the method generates reliable results. A natural progression is to compare the technique with a multi-input SSA (not available to the authors at the moment).

**Author Contributions:** Conceptualization, I.R. and K.C.; methodology, I.R.; software, I.R.; validation, I.R.; formal analysis, I.R.; investigation, I.R.; resources, I.R. and K.C.; data curation, I.R.; writing—original draft preparation, I.R.; writing—review and editing, K.C.; visualization, I.R.; supervision, K.C.; project administration, K.C.; funding acquisition, K.C. All authors have read and agreed to the published version of the manuscript.

**Funding:** This research was funded by POB HEP of Warsaw University of Technology within the Excellence Initiative: Research University (IDUB) programme.

**Institutional Review Board Statement:** Not applicable.

**Informed Consent Statement:** Not applicable.

**Data Availability Statement:** Not applicable.

**Conflicts of Interest:** The authors declare no conflict of interest.

## Abbreviations

The following abbreviations are used in this manuscript:

AM	Amplitude Modulation
DAC	Digital–Analog Converter
DC	Direct Current
DDS	Direct Digital Synthesizer
DUT	Device Under Test
FPGA	Field-Programmable Gate Array
IC	Integrated Circuit
JTF	Jitter Transfer Function
LFSR	Linear Feedback Shift Register
NCO	Numerically Controlled Oscillator
PLL	Phase Locked Loop
PM	Phase Modulation
PN	Phase Noise
PNTF	Phase Noise Transfer Function
SA	Spectrum Analyzer
SINAD	Signal-to-Noise And Distortion ratio
SSA	Signal Source Analyzer
VCO	Voltage–Controlled Oscillator

## References

1. Puglia, K.V. Phase noise analysis of component cascades. *IEEE Microw. Mag.* **2002**, *3*, 71–75. [[CrossRef](#)]
2. Egan, W.F. *Phase-Lock Basics*; John Wiley & Sons, Inc.: New York, NY, USA, 1998.
3. Rubiola, E. *Phase Noise and Frequency Stability in Oscillators*; Cambridge University Press: Cambridge, UK, 2008.
4. Gruson, Y.; Rus, A.; Rohde, U.L.; Roth, A.; Rubiola, E. Artifacts and errors in cross-spectrum phase noise measurements. In *Metrologia*; BIPM & IOP Publishing Ltd.: Bristol, UK, 2020; Volume 57, p. 055010. [[CrossRef](#)]
5. Brandon, D.; Cavey, J. The Residual Phase Noise Measurement. 2008. Available online: <https://www.analog.com/media/en/technical-documentation/application-notes/AN-0982.pdf> (accessed on 19 October 2021).
6. Gheen, K. *2-Port Residual Noise Measurements | 1EF100*; Rhode and Schwarz: Munich, Germany, 20 October 2017.
7. Rutkowski, I.; Czuba, K. Characterization of Frequency Converters' Phase Noise Transfer Function. In Proceedings of the 23rd International Microwave and Radar Conference (MIKON), Warsaw, Poland, 5–8 October 2020; pp. 1–4. [[CrossRef](#)]
8. Goldberg, B.-G. *Digital Frequency Synthesis Demystified: DDS and Fractional-N PLLs*; LLH Technology Publishing: Eagle Rock, VA, USA, 1999.
9. Schat, J.; Möhlmann, U. Concurrent Estimation of a PLL Transfer Function by Cross-Correlation with pseudo-random Jitter. In Proceedings of the 2019 IEEE European Test Symposium (ETS), Baden-Baden, Germany, 27–31 May 2019; pp. 1–2. [[CrossRef](#)]
10. George, M.; Alfke, P. Linear Feedback Shift Registers in Virtex Devices, Xilinx Application Note 210. 30 April 2007. Available online: [https://www.xilinx.com/support/documentation/application\\_notes/xapp210.pdf](https://www.xilinx.com/support/documentation/application_notes/xapp210.pdf) (accessed on 30 November 2021).